Reaction between $CH_3C(O)OOH$ (peracetic acid) and OH: A combined experimental and theoretical study of the kinetics and mechanism

Matias Berasategui[1], Damien Amedro[1], Luc Vereecken[2], Jos Lelieveld and John N. Crowley[1]

[1] Division of Atmospheric Chemistry, Max-Planck-Institut für Chemie, 55128 Mainz, Germany
[2 2] Institute for Energy and Climate Research: IEK-8, Forschungszentrum Juelich, 52425 Juelich, Germany

Correspondence to: John N. Crowley (john.crowley@mpic.de)

Supplementary Information

Table S1. Rate constants for the reaction OH (k_6) and OD (k_7) with $CH_3C(O)OH$ at 298 K.

Precursor	$[CH_3C(O)OH]$ [a]	[Precursor] [b]	$[OH]_0$ [c]	k' [d]	k_6 or k_7 [e]
H_2O_2 (OH)	0	19.42	6.47	472.67 ± 2.3	6.95 ± 0.08
	19.54 ± 1.20	19.42	6.48	1679.33 ± 6.2	
	24.70 ± 1.25	19.42	6.48	2016.66 ± 12.3	
	30.76 ± 1.31	19.41	6.47	2606.32 ± 9.2	
	36.82 ± 1.37	19.42	6.48	3046.21 ± 8.7	
	41.76 ± 1.04	19.42	6.47	3363.66 ± 10.6	
H_2O_2 (OH)	0	4.85	1.62	668.94 ± 10.4	7.04 ± 0.28
	17.75 ± 1.18	3.83	1.28	1930.14 ± 59.3	
	4.01 ± 1.04	3.33	1.11	986.54 ± 17.2	
	11.64 ± 1.17	2.99	1.00	1512.84 ± 30.4	
	18.51 ± 1.19	3.23	1.08	1972.35 ± 43.9	
	21.95 ± 1.22	2.99	1.00	2229.59 ± 35.0	
	24.81 ± 1.25	2.56	0.85	2393.95 ± 39.4	
DNO_3 (OD)	0	5.84	1.95	1129.54 ± 26.5	7.30 ± 0.26
	14.15 ± 1.14	5.95	1.98	2153.9 ± 58.2	
	9.88 ± 1.10	6.31	2.11	1865.88 ± 60.2	
	11.45 ± 1.11	5.95	1.99	1960.29 ± 48.0	
	16.17 ± 1.16	6.32	2.11	2312.91 ± 47.5	
	4.27 ± 1.04	5.88	1.96	1436.82 ± 43.0	

[a] in 10^{14} molecule cm^{-3} (errors are total uncertainty, 2σ).
[b] in 10^{14} molecule cm^{-3}.
[c] Calculated from $[H_2O_2]$ or $[DNO_3]$, in 10^{11} molecule cm^{-3}.
[d] First-order decay constant for OH or OD (s^{-1}).
[e] 10^{-13} cm^3 $molecule^{-1}$ s^{-1}.

Table S2. Reaction between OH or OD and $CH_3C(O)OOH$: Experimental conditions and Results.

Temp (K)	Precur-sor	$[CH_3C(O)OH]$ [a]	$[CH_3C(O)OOH]$ [b]	$[OH]_0$ [c]	$k_4'+k_6'+k_d$	k_6'	$k_4'+k_d$	k_4
298	PAA	12.8 ± 0.41	26.8 ± 2.87	13.4	1089 ± 5	904 ± 141	185±128	3.2 ± 0.6
		8.20 ± 0.47	16.7 ± 2.36	8.3	715 ± 3	579 ± 90	136±82	
		15.6 ± 0.39	35.7 ± 3.32	17.9	1337 ± 3	1102 ±172	235±156	
		14.5 ± 0.40	33.5 ± 3.21	16.8	1254 ± 4	1024 ±160	230±145	
		2.52 ± 0.58	6.17 ± 1.84	3.1	302 ± 2	178 ± 28	124±25	
		4.82 ± 0.53	11.6 ± 2.11	5.8	470 ± 3	340 ± 53	130±48	
306	PAA	8.62 ± 0.48	12.9 ± 2.17	6.4	744 ± 6	570 ± 89	174±81	4.3 ± 0.5
		20.2 ± 0.36	37.8 ± 3.42	18.9	1611 ± 12	1335 ± 209	276±189	
		13.0 ± 0.42	21.9 ± 2.63	10.9	1081 ± 8	859 ± 134	222±122	
		18.3 ± 0.37	32.5 ± 3.15	16.2	1459 ± 12	1210 ± 189	249±172	
		15.8 ± 0.40	28.0 ± 2.93	14.0	1299 ± 11	1044 ± 163	255±148	
316	PAA	8.49 ± 0.48	13.7 ± 2.22	6.9	665 ± 5	520 ± 81	145±74	3.7 ± 0.6
		20.2 ± 0.36	38.5 ± 3.45	19.2	1498 ± 9	1238 ± 193	260±175	
		12.8 ± 0.42	22.7 ± 2.66	11.3	1005 ± 6	784 ± 123	220±111	
		18.1 ± 0.38	32.6 ± 3.16	16.3	1322 ± 8	1109 ± 173	213±157	
		15.4 ± 0.40	28.8 ± 2.97	14.4	1160 ± 8	944 ± 147	217±134	
		3.90 ± 0.56	6.79 ± 1.87	3.4	377 ± 2	239 ± 37	138±34	
326	PAA	8.35 ± 0.49	14.4 ± 2.25	7.2	616 ± 6	478 ± 75	138±68	2.5 ± 0.8
		19.9 ± 0.38	37.8 ± 3.42	18.9	1400 ± 8	1140 ± 178	260±161	
		12.4 ± 0.45	22.9 ± 2.68	11.5	882 ± 8	710 ± 111	172±101	
		17.7 ± 0.40	33.2 ± 3.19	16.6	1226 ± 11	1014 ± 158	212±144	
		15.2 ± 0.41	29.1 ± 2.98	14.5	1061 ± 10	871 ± 136	190±124	
		4.70 ± 0.56	8.21 ± 1.94	4.1	421 ± 3	269 ± 42	152±38	
335	PAA	8.92 ± 0.49	14.9 ± 2.28	7.5	643 ± 7	481 ± 75	162±68	2.9 ± 0.6
		19.4 ± 0.39	37.3 ± 3.40	18.7	1321 ± 9	1046 ± 163	275±148	
		12.4 ± 0.44	20.7 ± 2.56	10.3	852 ± 11	669 ± 104	184±95	
		17.9 ± 0.39	32.3 ± 3.15	16.2	1195 ± 15	965 ± 151	229±137	
		15.8 ± 0.41	28.1 ± 2.93	14.0	1070 ± 10	852 ± 133	218±121	
		4.35 ± 0.54	7.96 ± 1.93	4.0	397 ± 7	235 ± 37	163±34	
345	PAA	8.91 ± 0.50	14.4 ± 2.25	7.2	589 ± 8	454 ± 71	135±65	3.5 ± 0.4
		19.3 ± 0.39	36.3 ± 3.35	18.2	1193 ± 13	983 ± 154	209±140	
		12.6 ± 0.45	22.5 ± 2.66	11.3	787 ± 11	642 ± 100	145±91	
		17.9 ± 0.40	31.9 ± 3.13	16.0	1104 ± 13	912 ± 142	192±130	
		15.7 ± 0.42	28.3 ± 2.95	14.2	995 ± 13	800 ± 125	195±114	
		5.66 ± 0.54	10.4 ± 2.05	5.2	406 ± 6	288 ± 45	118±41	
353	PAA	8.81 ± 0.50	14.8 ± 2.27	7.4	548 ± 16	429 ± 67	120±63	4.0 ± 0.4
		19.6 ± 0.39	35.5 ± 3.31	17.8	1155 ± 10	954 ± 149	201±135	
		12.8 ± 0.45	22.6 ± 2.66	11.3	776 ± 14	623 ± 97	154±89	
		17.3 ± 0.40	32.5 ± 3.16	16.3	1013 ± 10	842 ± 132	171±119	
		15.6 ± 0.42	28.4 ± 2.95	14.2	915 ± 15	759 ± 119	156±108	
		5.46 ± 0.57	8.83 ± 1.97	4.4	351 ± 8	266 ± 42	85±38	
298	$DONO_2$	12.6 ± 0.52	26.9 ± 2.87	2	1993 ± 41	890 ± 139	1104±132	4.3 ± 0.5
		8.89 ± 0.28	18.4 ± 2.45	2	1686 ± 36	628 ± 98	1058±96	
		15.8 ± 0.41	33.3 ± 3.20	2	2218 ± 54	1116 ±174	1102±167	
		29.4 ± 0.66	61.9 ± 4.63	2	3325 ± 71	2076 ± 324	1249±302	
		23.5 ± 0.64	49.0 ± 3.98	2	2862 ± 73	1659 ± 259	1202±246	

[a]Concentration of $CH_3C(O)OH$ in 10^{14} molecule cm^{-3}. [b]Concentration of $CH_3C(O)OOH$ in 10^{14} molecule cm^{-3} [c]OH concentration in 10^{11} molecule cm^{-3}.

Table S3. Reaction scheme used in the numerical simulations.

Reaction	**Rate coefficient**	**Reference**
$OH + CH_3COOH \rightarrow H_2O + CH_3 + CO_2$	$8.4 \times 10^{-20} T^2 \exp(1356/T)$	(IUPAC, 2020)
$OH + CH_3C(O)OOH \rightarrow H_2O + CH_3C(O)O_2$	varied	This work
$OH + CH_3 \rightarrow CH_3OH$	1.2×10^{-10}	(Sangwan et al., 2012)
$OH + CH_3C(O)O_2 = HO_2 + CH_3$	1×10^{-10}	By analogy to $OH + CH_3O_2$
$OH + HO_2 \rightarrow H_2O + O_2$	$4.8 \times 10^{-11}\exp(250/T)$	(IUPAC, 2020)
$HO_2 + HO_2 \rightarrow H_2O_2$	2.0×10^{-12}	(IUPAC, 2020)
$HO_2 + CH_3C(O)O_2 \rightarrow CH_3C(O)OOH + O_2$	$1.5 \times 10^{-12}\exp(480/T)$	(IUPAC, 2020)
$HO_2 + CH_3C(O)O_2 \rightarrow CH_3C(O)OH + O_3$	$4.4 \times 10^{-15}\exp(1910/T)$	(IUPAC, 2020)
$HO_2 + CH_3C(O)O_2 \rightarrow OH + CH_3 + CO_2$	$4.66 \times 10^{-12}\exp(235/T)$	(IUPAC, 2020)
$CH_3 + CH_3 \rightarrow C_2H_6$	5×10^{-11}	(Slagle et al., 1988)
$HO_2 + CH_3 \rightarrow CH_3O + OH$	3×10^{-11}	(Baulch et al., 2005)
$CH_3C(O)O_2 + CH_3C(O)O_2 \rightarrow 2\ CH_3 + 2\ CO_2 + O_2$	$2.9 \times 10^{-12}\exp(500/T)$	(IUPAC, 2020)[a]

[a]Assumes rapid decomposition of the initially formed $CH_3C(O)O$ radical.

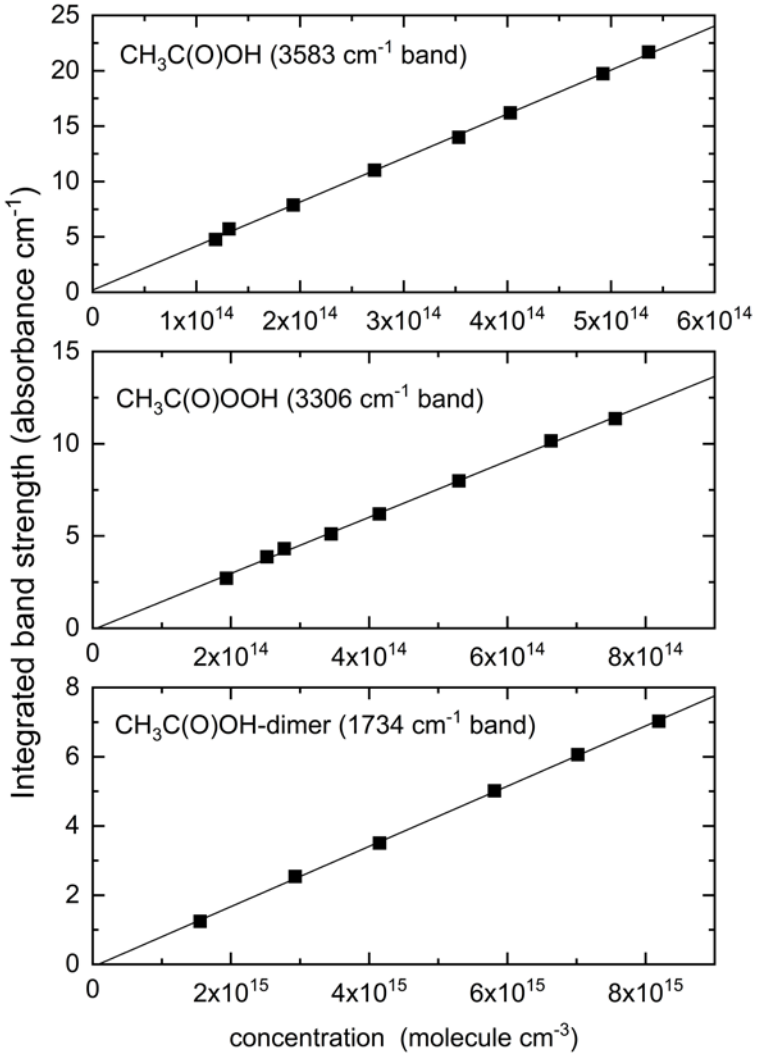

Figure S1. Beer-Lambert plots (integrated absorption over listed bands) versus concentration of $CH_3C(O)OH$, $CH_3C(O)OOH$ and $CH_3C(O)OH$-dimer.

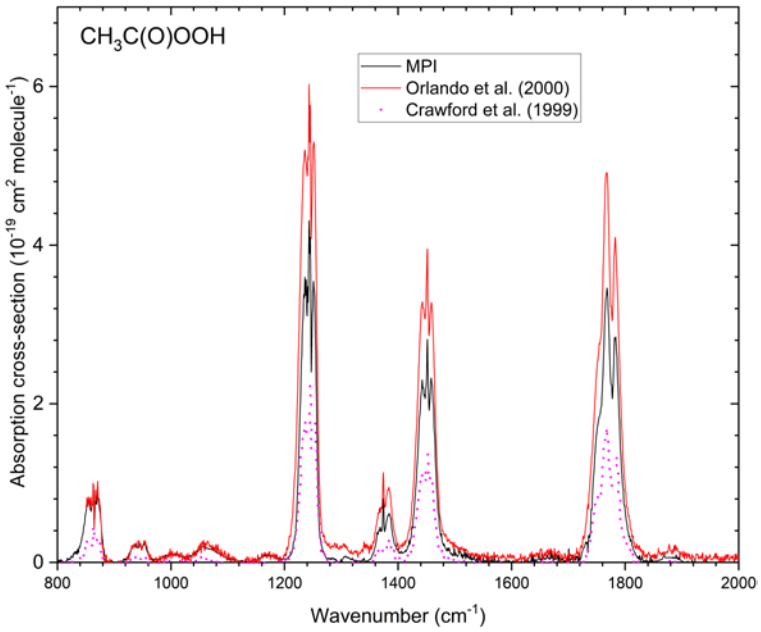

Figure S2. IR spectra of $CH_3C(O)OOH$ recorded in this work (MPI), and those published by Orlando et al. (2000) (who reported a single value at 1251 cm^{-1}) and Crawford et al. (1999). The spectrum of Crawford et al. was digitized from their Figure 2, that of Orlando et al. was kindly provided by the authors.

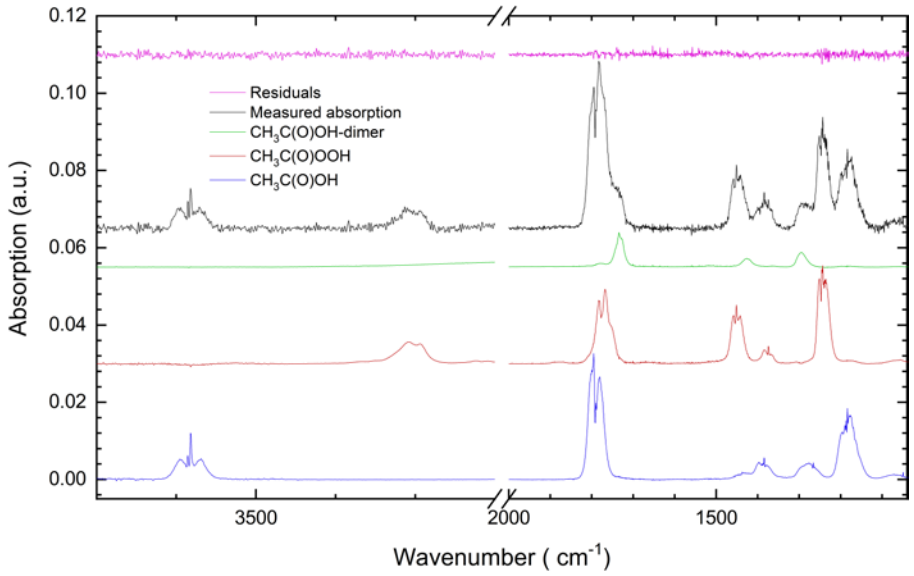

Figure S3. IR-absorption (black trace) measured during an experiment to determine k_4 at 298 K and 125 Torr N_2. The scaled reference spectra of $CH_3C(O)OOH$, $CH_3C(O)OH$ and $CH_3C(O)OH$-dimer as well as the residual obtained by subtraction are also displayed.

References

Baulch, D. L., Bowman, C. T., Cobos, C. J., Cox, R. A., Just, T., Kerr, J. A., Pilling, M. J., Stocker, D., Troe, J., Tsang, W., Walker, R. W., and Warnatz, J.: Evaluated kinetic data for combustion modeling: Supplement II, J. Phys. Chem. Ref. Data, 34, 757-1397, 2005.

IUPAC: Task Group on Atmospheric Chemical Kinetic Data Evaluation, (Ammann, M., Cox, R.A., Crowley, J.N., Herrmann, H., Jenkin, M.E., McNeill, V.F., Mellouki, A., Rossi, M. J., Troe, J. and Wallington, T. J.) http://iupac.pole-ether.fr/index.html., 2020. 2020.

Sangwan, M., Chesnokov, E. N., and Krasnoperov, L. N.: Reaction CH_3 + OH Studied over the 294-714 K Temperature and 1-100 bar Pressure Ranges, J. Phys. Chem. A, 116, 8661-8670, 2012.

Slagle, I. R., Gutman, D., Davies, J. W., and Pilling, M. J.: Study of the recombination reaction CH_3 + CH_3 -> C_2H_6. 1. Experiment, J. Phys. Chem., 92, 2455-2462, 1988.